Flavonoids from *Litsea japonica* Inhibit AGEs Formation and Rat Lense Aldose Reductase *In Vitro* and Vessel Dilation in Zebrafish

Authors Ik-Soo Lee[1], Yu Jin Kim[1], Seung-Hyun Jung[1], Joo-Hwan Kim[2], Jin Sook Kim[1]

Affiliations
[1] KM Convergence Research Division, Korea Institute of Oriental Medicine, Daejeon, Republic of Korea
[2] Department of Life Science, Gachon University, Seongnam, Republic of Korea

Key words
- *Litsea japonica*
- Lauraceae
- advanced glycation end-products
- rat lens aldose reductase
- zebrafish
- diabetic vascular complications

Abstract

In our ongoing efforts to identify effective naturally sourced agents for the treating of diabetic complications, two new (**1** and **2**) and 11 known phenolic compounds (**3**–**13**) were isolated from an 80% ethanol extract of *Litsea japonica* leaves. The structures of the new compounds were established by spectroscopic and chemical studies. These isolates (**1**–**13**) were subjected to an *in vitro* bioassay evaluating their inhibitory activity on advanced glycation end products formation and rat lens aldose reductase activity. Of the compounds evaluated, the flavonoids (**3, 4, 6**–**8, 11**, and **12**) markedly inhibited advanced glycation end products formation, with IC_{50} values of 7.4–72.0 µM, compared with the positive control, aminoguanidine (IC_{50} = 975.9 µM). In the rat lens aldose reductase assay, consistent with the inhibition of advanced glycation end products formation, the flavonoids (**3, 4, 6**–**8, 11**, and **12**) exhibited considerable inhibition of rat lens aldose reductase activity, with IC_{50} values of 1.1–12.5 µM. In addition, the effects of kaempferol (**4**) and tiliroside (**7**) on the dilation of hyaloid-retinal vessels induced by high glucose in larval zebrafish were investigated. Only kaempferol significantly reduced the diameters of high glucose-induced hyaloid-retinal vessels, by 52.2% at 10 µM, compared with those in the high glucose-treated control group.

Abbreviations

AGEs:	advanced glycation end products
AG:	aminoguanidine
AR:	Aldose reductase
DA:	dihydrodehydrodiconiferyl alcohol
HG:	high-glucose
RLAR:	rat lens aldose reductase
TMG:	3,3-tetramethyleneglutaric acid
VEGFR:	vascular endothelial growth factor receptor

received July 1, 2016
revised August 18, 2016
accepted August 26, 2016

Bibliography
DOI http://dx.doi.org/10.1055/s-0042-116324
Published online
Planta Med © Georg Thieme Verlag KG Stuttgart · New York · ISSN 0032-0943

Correspondence
Dr. Jin Sook Kim
KM Convergence Research Division
Korea Institute of Oriental Medicine
Daejeon 305–811
Republic of Korea
Phone: + 82 42 868 946
Fax: + 82 42 868 9471
jskim@kiom.re.kr

Introduction

Diabetic vascular complications are a leading cause of acquired blindness, renal failure, and nerve damage. Chronic hyperglycemia is fundamental for the development and progression of diabetic vascular complications through various hyperglycemia-induced metabolic derangements, including increased AGEs formation, increased polyol pathway flux, activation of protein kinase C isomers, and increased hexosamine pathway flux [1–3]. AGEs, the products of nonenzymatic glycation and oxidation of proteins and lipids, have been recognized as important pathogenetic mediators in diabetes-related complications. The accumulation of AGEs causes structural and functional changes in proteins such as collagen, elastin, and albumin and leads to the development and progression of numerous complications associated with diabetes, such as neuropathy, nephropathy, angiopathy, and retinopathy [4]. AR (alditol/$NADP^+$ oxidoreductase, E.C.1.1.1.21) is the key enzyme of the polyol pathway that catalyzes the NADPH-dependent reduction of glucose to sorbitol. Under diabetic conditions, elevated glucose levels enhance AR activity by increasing glucose flux through the polyol pathway, which induces functional and morphological changes associated with diabetic complications, such as cataracts, retinopathy, neuropathy, and nephropathy [5,6]. Thus, the development of pharmacological agents that inhibit AGEs formation or AR activity might provide a therapeutic approach to delay or prevent diabetic complications [7,8].
Medicinal plants, which are likely to be nontoxic, may be useful for the prevention and treatment of

diabetes-related complications. *Litsea japonica* (Thunb.) Juss. (Lauraceae) is an evergreen tree that grows in the southern parts of Korea, Japan, and China. Previous phytochemical studies on this plant resulted in the isolation of a number of essential oils, fatty acids, alkaloids, lactones, anthocyanins, and terpenoids [9–14]. Recently, it was reported that a crude extract from the leaves of *L. japonica* induced apoptosis of HL-60 leukemia cells [15] and significantly inhibited complement activity *in vitro* [16]. In our ongoing efforts to identify effective, naturally sourced therapeutic agents for diabetic complications, we found that an extract from *L. japonica* reduced the development of diabetic nephropathy via the inhibition of AGEs formation in db/db mice [17] and prevented diabetes-induced lens opacification via the inhibition of AR activity [18]. However, the active compounds underlying these effects of *L. japonica* remain unknown. Further phytochemical studies of this plant resulted in the isolation of two new (**1** and **2**) and 11 known compounds (**3**–**13**). In this report, we describe the isolation and structural elucidation of these compounds, as well as the characterization of their inhibitory effects on AGEs formation and RLAR activity. The effects of kaempferol (**4**) and tiliroside (**7**) on the dilation of HG-induced hyaloid-retinal vessels in larval zebrafish were also investigated.

Results and Discussion

An 80% ethanol extract of *L. japonica* leaves was suspended in water and partitioned successively using *n*-hexane, EtOAc, and *n*-BuOH. The EtOAc-soluble fraction that significantly inhibited both AGEs formation (IC_{50} = 8.5 µg/mL) and RLAR activity (IC_{50} = 2.3 µg/mL) was subjected to a series of chromatographic techniques. This led to the isolation of two new (**1** and **2**) and 11 known compounds (**3**–**13**; ◉ **Fig. 1**). By comparing their physicochemical and spectral data with those in literature, the 11 known compounds were identified as epicatechin (**3**) [16], kaempferol (**4**) [19], afzelin (**5**) [16], rhamnocitrin-3-*O*-rhamnoside (**6**) [20], tiliroside (**7**) [16], kaempferol 3-*O*-rutinoside (**8**) [21], quercitrin (**9**) [16], rutin (**10**) [16], quercetin 3-*O*-*β*-D-apiofuranosyl-(1 → 2)-*β*-D-glucopyranoside (**11**) [22], myricitrin (**12**) [16], and lyoniside (**13**) [23].

Compound **1** was obtained as a white amorphous powder with a negative specific rotation, $[\alpha]_D^{25}$ −43.0 (*c* 0.1, MeOH). HRESI-MS analysis of **1** yielded a molecular ion peak at *m/z* 537.1964 $[M + H]^+$, in accordance with the molecular formula $C_{26}H_{32}O_{12}$. The UV absorption maxima of **1** in MeOH observed at 276 nm suggested the presence of aromatic ring(s). Acid hydrolysis of **1** yielded an aglycone and a monosaccharide unit. The ^{1}H NMR spectrum (◉ **Table 1**) of the aglycone unit displayed five aromatic protons, including two *meta*-coupled doublets [δ_H 6.77 (1H, d, *J* = 2.0 Hz) and 6.73 (1H, d, *J* = 2.0 Hz)] and ABX aromatic system protons [δ_H 7.13 (1H, d, *J* = 8.4 Hz), 7.02 (1H, d, *J* = 2.0 Hz), and 6.92 (1H, dd, *J* = 8.0, 2.0 Hz)], a pair of hydroxymethylene protons [δ_H 3.74 (1H, dd, *J* = 11.0, 7.5 Hz) and 3.70 (1H, dd, *J* = 11.0, 4.0 Hz)], and two methoxyl protons [δ_H 3.82 and 3.86 (each 3H, s)], in addition to aliphatic peaks corresponding to a dihydroconiferylic acid side chain and a dihydrobenzofuran ring. These spectroscopic data suggested that **1** is a dihydrobenzofuran-type neolignan, after comparing with reported analogs [24,25]. This proposed skeleton was supported by the ^{13}C-NMR spectrum (◉ **Table 1**), which revealed two carbon signals at δ_C 88.63 (C-7) and 55.85 (C-8) characteristic of a dihydrobenzofuran neolignan. These spectroscopic data were similar to those for DA [24], except for the resonance of a carboxyl group (δ_C 179.72) instead of a hydroxymethylene group at C-9′ in DA, suggesting that the dihydroconiferyl alcohol group of DA was replaced by a dihydroconiferylic acid group in **1**. The presence of a dihydroconiferylic acid moiety in **1** was further confirmed by the ^{1}H-^{1}H COSY correlations between H-7′ [δ_H 2.85 (2H, t, *J* = 7.7 Hz)] and H-8′ [δ_H 2.49 (2H, t, *J* = 7.8 Hz)], together with the HMBCs of both H-7′ and H-8′ with a carboxyl carbon signal (δ_C 179.72; ◉ **Fig. 2**). The attachment of this moiety at C-1′ was deduced from the HMBC experiment. The six carbon signals at δ_C 102.89, 78.32, 77.97, 75.04, 71.45, and 62.58 and an anomeric proton signal at δ_H 4.87 of **1** were typical of a glucose unit, which was identified as D-glucose, followed by GC analysis of the acid hydrolysate. Moreover, the large coupling constant (*J* = 7.5 Hz) of the anomeric proton indicated that the glucose unit was linked in a *β*-configuration. The location of a glucose unit at C-4 was elucidated from the HMBC between the anomeric proton signal at δ_H 4.87 (H-1″) and the aglycone carbon signal at δ_C 147.73 (C-4; ◉ **Fig. 2**). The large coupling constant (*J* = 6.4 Hz) between H-7 and H-8 indicated the relative *trans*-vicinal coupling of the dihydrobenzofuran ring. This was confirmed by the cross peaks observed between H-7 and H-9b and between H-8 and H-6 in the NOESY spectrum (◉ **Fig. 3**). The absolute configuration at C-7 and C-8 was determined to be 7*S*,8*R* from the circular dichroism spectrum of **1**, showing a positive Cotton effect in the region of 270–290 nm, compared with those reported for dihydrobenzofuran lignans [26,27]. Thus, the structure of **1** was determined to be (7*S*,8*R*)-dihydrodehydrodiconiferylic acid 4-*O*-*β*-D-glucopyranoside.

Compound **2** was obtained as a white powder with the molecular formula $C_{22}H_{28}O_{10}$, as established by HRESI-MS, based on a molecular ion peak at *m/z* 453.1753 $[M + H]^+$. Its UV absorption maxima (282, 315, 330 nm) suggested the presence of a naphthalene nucleus [28], which was supported by the analysis of the ^{1}H- and ^{13}C-NMR spectra (◉ **Table 2**). The ^{13}C-NMR spectrum, together with the DEPT data, showed that **2** contained 22 carbons, 10 of which were consistent with those of a 1-naphthol unit [29]. The 12 remaining signals were assigned to glucose (δ_C 102.86, 78.38, 77.18, 75.22, 71.76, and 68.09) and rhamnose (δ_C 102.35, 74.17, 72.55, 72.33, 70.01, and 18.06) units, which were identified as D-glucose and L-rhamnose, respectively, by GC analysis of the acid hydrolysate. The *β*-configuration of the glucose unit was confirmed by the coupling constant of the anomeric proton at δ_H 5.04 (1H, d, *J* = 7.8 Hz), and the α-configuration of the rhamnose unit was determined by the anomeric proton at δ_H 4.71 (1H, d, *J* = 1.5 Hz). The HMBC correlation between H-1″ (δ_H 4.71) and C-6′ (δ_C 68.09) indicated a rhamnopyranosyl-(1 → 6)-glucopyranosyl linkage (◉ **Fig. 2**). Furthermore, the attachment of the sugar chain at C-1 on the 1-naphthol structure was deduced from the HMBC spectrum, showing HMBC correlations between H-1′ (δ_H 5.04) and the aglycone carbon C-1 (δ_C 154.73; ◉ **Fig. 2**). Thus, the glycoside linkage was identified as α-L-rhamnopyranosyl-(1 → 6)-*O*-*β*-D-glucopyranosyl located at C-1 of the aglycone. Finally, the structure of **2** was established as 1-naphthol 1-*O*-α-L-rhamnopyranosyl-(1 → 6)-*O*-*β*-D-glucopyranoside.

Previously, we reported that some phenolic compounds, such as afzelin (**5**), quercitrin (**9**), and rutin (**10**), exhibit considerable inhibitory effects on AGEs formation and RLAR [30]. In this study, we further investigated the inhibitory effects of isolated compounds, apart from the previously evaluated compounds, on AGEs formation and RLAR activity *in vitro* (◉ **Table 3**). Of the compounds evaluated, flavonoids, epicatechin (**3**), kaempferol (**4**), rhamnocitrin-3-*O*-rhamnoside (**6**), tiliroside (**7**), kaempferol

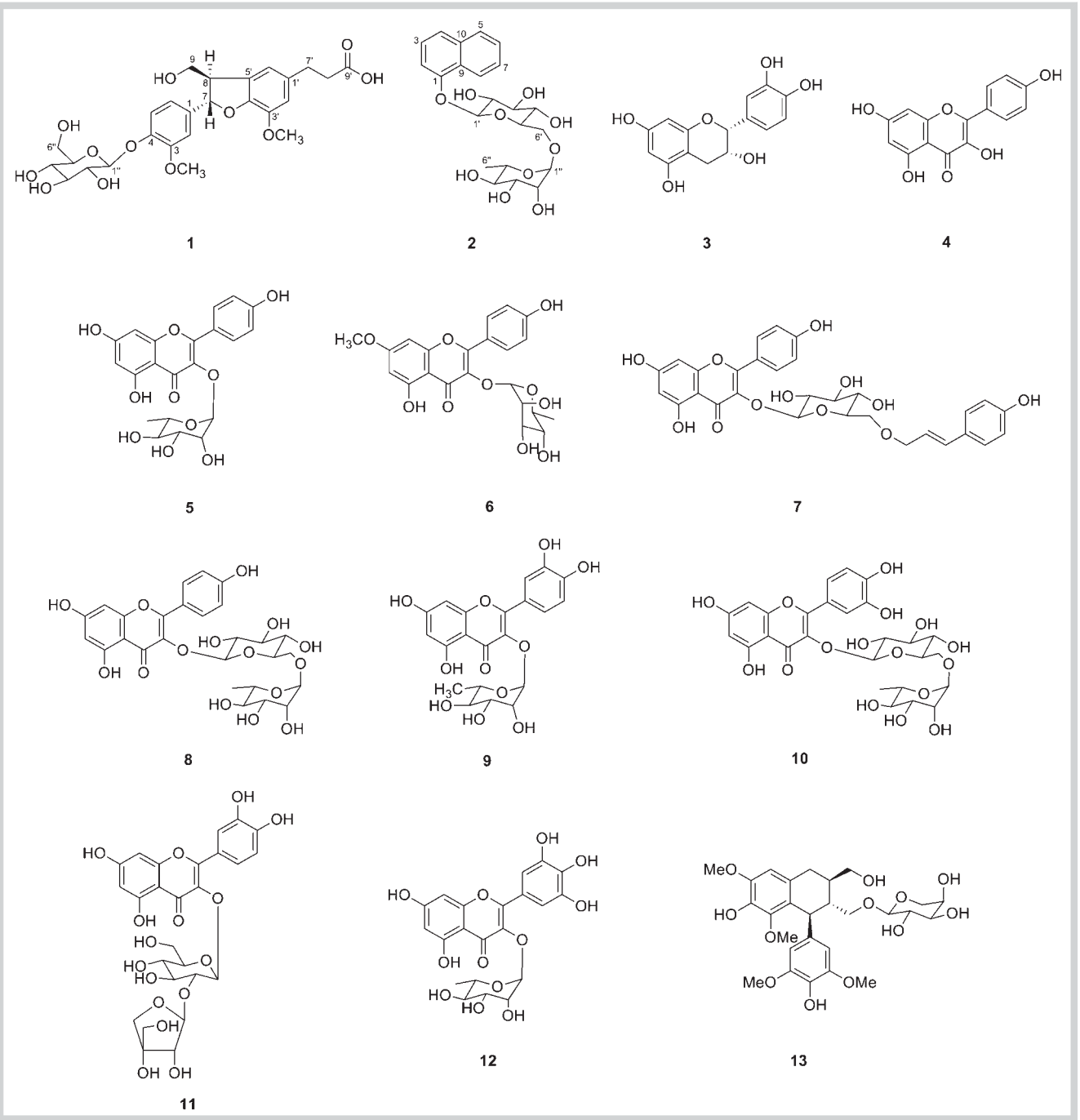

Fig. 1 Chemical structures of compounds **1**–**13** from *L. japonica*.

3-*O*-rutinoside (**8**), quercetin 3-*O*-*β*-D-apiofuranosyl-(1 → 2)-*β*-D-glucopyranoside (**11**), and myricitrin (**12**) markedly inhibited AGEs formation, with IC_{50} values of 7.4–72.0 µM, compared with the positive control AG (IC_{50} = 975.9 µM), the first AGEs inhibitor used for the treatment of diabetic nephropathy [31]. On the other hand, the other four isolates, including two new compounds (**1** and **2**), did not exhibit any significant activity. In the RLAR assay, consistent with the inhibition of AGEs formation, flavonoids (**3, 4, 6**–**8, 11**, and **12**) exhibited considerable inhibition of RLAR, with IC_{50} values of 1.1–12.5 µM. Of the active compounds, kaempferol (**4**) and tiliroside (**7**) exhibited greater inhibitory effects on RLAR, with IC_{50} values of 1.1 and 3.4 µM, respectively, than those exhibited by the positive control, TMG (IC_{50} = 4.1 µM). Zebrafish has been used extensively for drug screening and as a model organism to analyze early and late diabetic complications [32]. Thus, kaempferol (**4**) and tiliroside (**7**), which potently inhibited both AGEs formation and RLAR activity, were investigated for their effects on retinopathy in diabetic zebrafish *in vivo*. The change in hyaloid-retinal vessel dilation was assessed in transgenic zebrafish embryos expressing EGFP in the vasculature (*flk*: EGFP) under HG (130 mM) conditions. In a toxicity test, compounds **4** and **7** were not toxic at concentrations up to 10 µM in the zebrafish (data not shown). Thus, to evaluate the effects of **4**

and **7** on the HG-induced dilation of hyaloid-retinal vessels, *flk:* EGFP transgenic zebrafish embryos were treated with these compounds at 5 and 10 µM. As shown in **Fig. 4**, only kaempferol significantly reduced the diameters of HG-induced hyaloid-retinal vessels by approximately 52% at 10 µM compared with those in the HG-treated control group, whereas the positive control, a VEGFR inhibitor, exhibited a 77% reduction at 1 µM. These results suggest that kaempferol inhibits the development of experimental retinopathy during the early larval stages.

In the current study on effective agents for diabetic complications derived from *L. japonica* leaves, several flavonoids were isolated. These flavonoids displayed considerable inhibition of both AGEs formation (IC_{50} 7.4–72.0 µM) and RLAR activity (IC_{50} 1.1–12.5 µM). Among the isolated flavonoids, kaempferol (**4**) significantly reduced the dilation of HG-induced hyaloid-retinal vessels in a diabetic zebrafish model. Flavonoids, a large group of naturally occurring polyphenolic compounds with a benzo-γ-pyrone structure, are widespread throughout the plant kingdom; various plants used in traditional medicine also contain significant amounts of these compounds. They have low toxicity and a variety of pharmacological activities, including antiallergic, antibacterial, antidiabetic, anti-inflammatory, antiviral, antiproliferative, hepatoprotective, estrogenic, insecticidal, and antioxidant effects [33]. However, due to the low bioavailability of flavonoids, they have not yet been approved as therapeutic agents. Indeed, low water solubility and stability, poor absorption, and extensive and rapid metabolic bioconversion contribute to the low bioavailability of flavonoids [34]. Therefore, further investigation is required to improve the bioavailability and subsequent efficacy of active flavonoids using medicinal chemistry approaches.

Materials and Methods

General experimental procedures

Optical rotations were measured using the JASCO P-2000 digital polarimeter. UV and CD spectra were recorded using JASCO V-550 UV/VIS and JASCO J-715 spectrometers, respectively. ^{1}H-NMR (300 MHz) and ^{13}C-NMR (75 MHz) spectra were obtained using a Bruker DRX-300 spectrometer with tetramethylsilane as an internal standard. Two-dimensional NMR experiments (COSY, HMBC, and NOESY) were performed on a Bruker Avance 500 NMR spectrometer. HRESI-MS was performed using a Shimadzu LCMS-IT-TOF spectrometer. Column chromatography was performed using silica gel (70–230 mesh and 230–400 mesh, Merck) and YMC-gel ODS-A (S-75 µm, YMC). Thin-layer chromatography was performed on pre-coated silica gel 60 F_{254} (0.25 mm, Merck) and RP-18 F_{254s} plates (0.25 mm, Merck). Spots were detected by UV light (254 nm) and spraying of 10% H_2SO_4 followed by heating.

Plant material

The leaves of *L. japonica* were collected in Gimnyeong-ri, Gujwa-eup, Jeju-si, Jeju-do, South Korea in March 2011 and identified by Prof. J-H. Kim, Gachon University, South Korea. A voucher specimen (DiAB-2008–061) has been deposited in the Herbarium of the Institute of Oriental Medicine, South Korea.

Extraction, fractionation, and isolation

The air-dried leaves of *L. japonica* (6.1 kg) were extracted using 80% aqueous ethanol (three times with 30 L each) at room temperature for 7 days, filtered, and concentrated to give an 80%

Table 1 ^{1}H (300 MHz), ^{13}C NMR (75 MHz), and HMBC data for compound **1** (in CD_3OD).

C	δ_c	δ_H (*J* in Hz)	HMBC (H→C)
1	138.52		
2	111.28	7.02 d (2.0)	151.05, 147.71, 138.52, 119.52, 88.63
3	151.05		
4	147.73		
5	118.15	7.13 d (8.4)	151.05, 147.73, 138.52
6	119.52	6.92 dd (8.4, 2.0)	147.73, 111.28, 88.63
7	88.63	5.56 d (6.4)	147.73, 138.52, 129.63, 119.52, 111.28, 65.14, 55.85
8	55.85	3.44 ddd (7.5, 6.4, 4.0)	147.73, 138.52, 129.63, 117.95, 88.63, 65.14
9	65.14	3.74 dd (11.0, 7.5), 3.70 dd (11.0, 4.0)	129.63, 88.63, 55.85
1′	129.63		
2′	114.17	6.77 d (2.0)	147.71, 145.38, 117.95, 33.07
3′	145.38		
4′	147.71		
5′	136.86		
6′	117.95	6.73 d (2.0)	147.71, 145.38, 114.17, 55.85, 33.07
7′	33.07	2.85 t (7.7)	179.72, 136.86, 117.95, 114.17, 39.74
8′	39.74	2.49 t (7.8)	179.72, 136.86, 33.07
9′	179.72		
1′′	102.89	4.87 d (7.5)	147.71
2′′	75.04	3.48 m	102.89, 77.97
3′′	77.97	3.46 m	75.04, 71.45
4′′	71.45	3.39 m	77.97
5′′	78.32	3.38 m	
6′′	62.58	3.84 m	88.63, 71.45, 55.85
		3.67 br d (10.30)	78.32, 71.45
3-OMe	56.85	3.82 s	151.05
3′-OMe	56.83	3.86 s	145.38

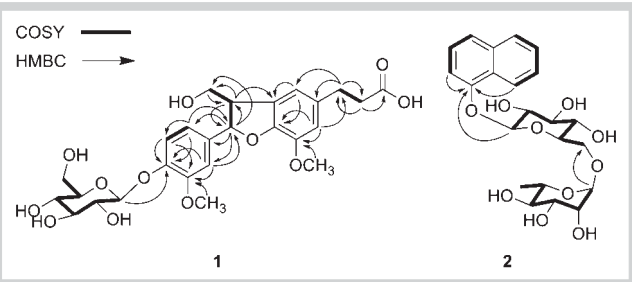

Fig. 2 Key ^{1}H-^{1}H COSY and HMBC correlations of compounds **1** and **2**.

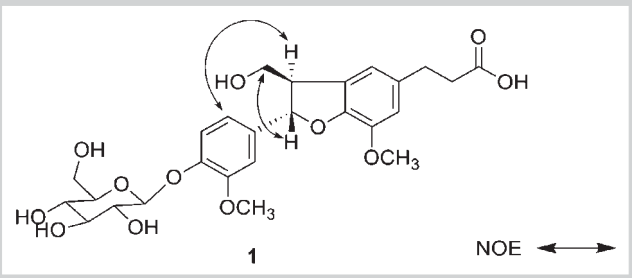

Fig. 3 Key NOE correlations of **1**.

ethanol extract (800 g). This extract (500 g) was suspended in water (4 L) and partitioned successively using *n*-hexane (3 × 4 L), EtOAc (3 × 4 L), and *n*-BuOH (3 × 4 L) to afford *n*-hexane- (144.2 g), EtOAc- (64.8 g), and *n*-BuOH-soluble fractions (116.3 g), respectively. The EtOAc-soluble fraction (62.3 g), which significantly inhibited both AGEs formation and RLAR activity, was subjected to silica gel column chromatography (70–230 mesh, 40 × 10 cm) and eluted with a gradient solvent system consisting of $CHCl_3$-MeOH (50 : 1, 30 : 1, 10 : 1, 5 : 1, 1 : 1, 0 : 1, 2 L each) to afford four fractions [A (2 L, 10.8 g), B (2 L, 8.3 g), C (4 L, 30.7 g), and D (4 L, 2.8 g)]. Fraction D (2.8 g) was subjected to YMC RP-18 column chromatography (50 × 5 cm) and eluted with a MeOH-H_2O gradient (1 : 10, 1 : 5, 1 : 0, 0.5 L each) to afford three subfractions [D1 (0.5 L, 0.8 g), D2 (0.5 L, 0.9 g), and D3 (0.5 L, 0.8 g)]. Subfraction D2 (0.9 g) was subjected to further chromatography using a YMC RP-18 column (50 × 3 cm) and a MeOH-H_2O gradient (1 : 10, 1 : 5, 1 : 2, 1 : 1, 0.5 L each) to obtain **1** (8 mg) and **2** (7 mg). Chromatography of fraction C (30.7 g) on a silica gel column (70–230 mesh, 50 × 10 cm), eluting with a $CHCl_3$-MeOH gradient (50 : 1, 30 : 1, 10 : 1, 5 : 1, 1 : 1, 0 : 1, 2 L each), afforded six fractions [C1 (2 L, 3.2 g), C2 (2 L, 3.5 g), C3 (2 L, 3.2 g), C4 (2 L, 2.3 g), C5 (2 L, 3.5 g), and C6 (2 L, 3.8 g)]. Fraction C3 (3.2 g) was further purified on a YMC RP-18 column (50 × 5 cm) using a MeOH–H_2O gradient (1 : 1, 2 : 1, 4 : 1, 6 : 1, 0.7 L each) to obtain **3** (197 mg), **4** (15 mg), and **5** (35 mg). Chromatography of fraction C5 (3.5 g) on a YMC RP-18 column (50 × 5 cm) using a MeOH-H_2O gradient (1 : 1, 2 : 1, 3 : 1, 4 : 1, 0.7 L each) afforded four fractions [C5.1 (0.7 L, 0.5 g), C5.2 (0.7 L, 0.8 g), C5.3 (0.7 L, 0.8 g), and C5.4 (0.7 L, 0.6 g)], one of which, C5.3 (0.8 g), was further chromatographed on a YMC RP-18 column (40 × 5 cm), eluting with a MeOH–H_2O gradient (2 : 1, 4 : 1, 6 : 1, 8 : 1, 10 : 1, 0.5 L each) to obtain **6** (119 mg), **7** (350 mg), **8** (9 mg), and **9** (21 mg). Fraction A (10.8 g) was subjected to silica gel column chromatography (70–230 mesh, 50 × 5 cm) using a $CHCl_3$-EtOAc gradient (50 : 1, 30 : 1, 10 : 1, 5 : 1, 1 : 1, 0 : 1, each 2 L) to afford three fractions [A1 (2 L, 1.2 g), A2 (4 L, 2.5 g), and A3 (6 L, 5.8 g)]. Subfraction A3 (5.8 g) was further chromatographed on a YMC RP-18 column (50 × 5 cm), eluting with a MeOH–H_2O gradient (2 : 1, 4 : 1, 6 : 1, 8 : 1, 10 : 1, 0.5 L each), to afford four subfractions [A3.1 (0.5 L, 0.5 g), A3.2 (0.5 L, 0.6 g), A3.3 (1 L, 2.1 g), and A3.4 (0.5 L, 0.8 g)]. Subfraction A3.3 (2.1 g) was chromatographed separately on a YMC RP-18 column (40 × 3 cm), eluting with a MeOH-H_2O gradient (1 : 1, 2 : 1, 3 : 1, 4 : 1, 5 : 1, 0.5 L each), to yield **10** (5 mg), **11** (9 mg), **12** (10 mg), and **13** (32 mg).

(7S,8R)-dihydrodehydrodiconiferylic acid 4-O-β-D-glucopyranoside (**1**): white powder; $[\alpha]_D^{25}$ −43.0 (*c* 0.1, MeOH); UV (MeOH) λ_{max} 230, 276 nm; CD (MeOH) $\Delta\varepsilon$ (nm) +2.5 (275), +6.8 (290); ^{1}H- and ^{13}C-NMR, see **Table 1**; HRESIMS *m/z* 537.1964 $[M + H]^+$ (calcd. for $C_{26}H_{33}O_{12}^+$, 537.1967).

1-Naphtol 1-O-α-L-rhamnopyranosyl-(1 → 6)-O-β-D-glucopyranoside (**2**): white powder; $[\alpha]_D^{25}$ −15.0 (*c* 0.1, MeOH); UV (MeOH) λ_{max} 282, 315, 330 nm; ^{1}H- and ^{13}C-NMR, see **Table 2**; HRESIMS *m/z* 453.1753 $[M + H]^+$ (calcd. for $C_{22}H_{29}O_{10}^+$, 453.1755)

Table 2 ^{1}H (300 MHz), ^{13}C-NMR (75 MHz), and HMBC data for compound **2** (in CD_3OD).

C	δ_c	δ_H	HMBC (H → C)
1	154.73		
2	110.76	7.19 dd (8.1, 2.3)	154.73, 127.45, 123.28
3	127.09	7.41 dd (8.1, 8.0)	154.73, 136.16, 127.45, 110.76
4	123.28	7.52 dd (8.0, 2.3)	154.73, 136.16, 128.5, 127.45, 110.76
5	128.57	7.80 dd (8.1, 8.0)	154.73, 136.16, 126.49, 123.28
6	127.47	7.47 m	136.16, 128.57, 127.45, 123.43, 123.28
7	126.49	7.45 m	136.16, 128.57, 127.45, 123.43, 123.28
8	123.43	8.37 dd (8.1, 2.3)	154.73, 136.16, 127.45
9	127.45		
10	136.16		
1′	102.86	5.04 d (7.80)	154.73, 78.38, 75.22
2′	75.22	3.65 m	102.86, 71.76, 68.09
3′	77.18	3.61 m	78.38
4′	71.76	3.43 m	78.38, 77.18, 68.09
5′	78.38	3.51 t (9.0)	102.86, 75.22, 71.76
6′	68.09	3.62 m, 4.05 d (9.4)	102.35, 77.18, 71.76
1′′	102.35	4.71 d (1.5)	72.33, 70.01
2′′	72.33	3.85 q (1.60)	74.17, 72.55
3′′	72.55	3.71 dd (9.5, 3.3)	74.17, 72.33
4′′	74.17	3.35 t (9.3)	72.33, 70.01, 18.06
5′′	70.01	3.66 m	68.09, 18.06
6′′	18.06	1.18 d (6.2)	74.17, 70.01

Table 3 Inhibitory effects of compounds from L. japonica against AGEs formation and RLAR.

Compound	IC_{50} (95% CI) μM[a]	
	AGEs Formation[b]	RLAR
1	> 100	> 100
2	> 100	> 100
3	67.2 (65.8–68.6)	10.8 (9.9–11.7)
4	32.1 (30.5–33.7)	1.1 (0.4–1.8)
6	60.9 (60.2–61.6)	12.5 (11.3–13.7)
7	7.4 (7.2–7.6)	3.4 (3.3–3.5)
8	72.0 (71.0–73.0)	11.3 (8.9–13.7)
11	25.0 (23.0–25.0)	7.9 (7.0–8.8)
12	33.3 (32.5–34.1)	4.8 (4.2–5.4)
13	> 100	> 100
AG[c]	975.9 (961.3–990.5)	–
TMG[c]	–	4.1 (4.0–4.2)

[a]Results are expressed as IC_{50} values and 95% confidence intervals (95% CI). IC_{50} indicates the concentration (μM) at which the inhibition percentage of the AGEs formation or RLAR was 50%. Values were determined by regression analysis using GraphPad 5.0 Prism software; [b]After incubating for 7 days, the fluorescent reaction products were assayed on a spectrofluorometric detector; [c]AG and TMG were used as positive controls.

Acid hydrolysis of 1 and 2

Compounds **1** and **2** (2 mg each) in 10% HCl/dioxane (1 : 1, 1 mL) were heated separately at 80 °C for 3 h in a water bath. The mixture was neutralized with Ag_2CO_3, filtered, and then extracted with EtOAc (20 mL). The aqueous layer was evaporated, and the residue was treated with L-cysteine methyl ester hydrochloride (2 mg) in pyridine (0.5 mL) at 60 °C for 1 h. After the reaction was completed, the solution was treated with acetic anhydride (3 mL) at 60 °C for 1 h. Authentic samples were prepared using the same procedure. The acetate derivatives were then subjected to GC analysis. GC conditions: GC-2010 (Shimadzu) instrument; detector, FID; column, TC-1 capillary column (0.25 mm × 30 m; GL Sciences, Inc.); column temperature, 230 °C; programmed increase, 38 °C/min; carrier gas, N_2 (1 mL/min); injection and detector

temperature, 270 °C. D-Glucose (t_R 16.31 min) was detected from **1** and **2**, and L-rhamnose (t_R 10.16 min) was detected from **2**.

Inhibition of AGEs formation assay

In accordance with a well-established method, a reaction mixture of bovine serum albumin (10 mg/mL, 700 µL; Sigma) in 50 mM phosphate buffer (pH 7.4) with 0.02 % sodium azide was added to 0.2 M fructose and glucose (100 µL). In screw-cap tubes (1.5 mL), the reaction mixture was then mixed with 200 µL of serially diluted compounds or AG (99 % purity; Sigma). After incubating at 37 °C for 7 days, the fluorescent reaction products (200 µL) were transferred to 96-well plates and assayed on a spectrofluorometric detector (Synergy HT; excitation wavelength, 350 nm, emission wavelength, 450 nm). The AGEs assay was performed in triplicate. The IC_{50} values and their 95 % confidence intervals were obtained by regression analysis using the GraphPad 5.0 Prism software.

RLAR inhibitory assay

All experimental protocols for animal care and use were approved by the local ethics board (South Korean Institute of Oriental Medicine Animal Care and Use Committee; Approval date and number: March 20, 2013 and 13–018, respectively), and animal husbandry and procedures were performed in accordance with institutional guidelines. Rat lenses were removed from the eyes of 8-week-old Sprague-Dawley rats (Dae-Han Bio Link Co.) weighing 100–150 g and homogenized in 12 volumes of 135 mM Na/K phosphate buffer (pH 7.0) containing 0.5 mM phenylmethylsulfonyl fluoride and 10 mM 2-mercaptoethanol. The homogenate was centrifuged at 100 000 × *g* for 30 min, and the supernatant was used to evaluate the crude RLAR. The incubation mixture contained 135 mM Na/K phosphate buffer (pH 7.0), 100 mM lithium sulfate, 0.03 mM NADPH, 1 mM DL-glyceraldehyde as a substrate, and 50 µL of the enzyme fraction, with or without 25 µL of the sample solution, in a total volume of 1.0 mL. The reaction was initiated by the addition of NADPH at 37 °C and stopped by the addition of 0.3 mL 0.5 M HCl. Then, 1 mL 6 M NaOH containing 10 mM imidazole was added, and the solution was heated at 60 °C for 10 min to convert NADP into a fluorescent product. Fluorescence was measured using a spectrofluorometric detector (Shimadzu RF-5301PC; excitation: 360, emission: 460 nm). The RLAR assay was performed in triplicate. The IC_{50} values and their 95 % confidence intervals were obtained by regression analysis using the GraphPad 5.0 Prism software. TMG (99 % purity; Sigma) was used as a positive control.

Measurement of vessel dilation in larval zebrafish

All experimental protocols for animal care and use were approved by the local ethics board (South Korean Institute of Oriental Medicine Animal Care and Use Committee; Approval date and number: April 10, 2013 and 13–022, respectively), and animal husbandry and procedures were performed in accordance with institutional guidelines. Adult zebrafish were maintained under standard conditions at 28.5 °C under a 14 h light/10 h dark cycle. Embryos were obtained from crosses between *flk*:EGFP transgenic fish and raised in egg water (sea salt, 0.06 g/L). One-day-old *flk*:EGFP embryos were placed in a 24-well plate (five embryos per well) and maintained in 2 mL egg water containing 130 mM glucose. HG-induced embryos were treated with **4** and **7** (5 or 10 µM) from 1 to 6 days post-fertilization (dpf). At 6 dpf, HG-induced embryos were fixed with 4 % paraformaldehyde, and the lens containing the hyaloid-retinal vessels was isolated.

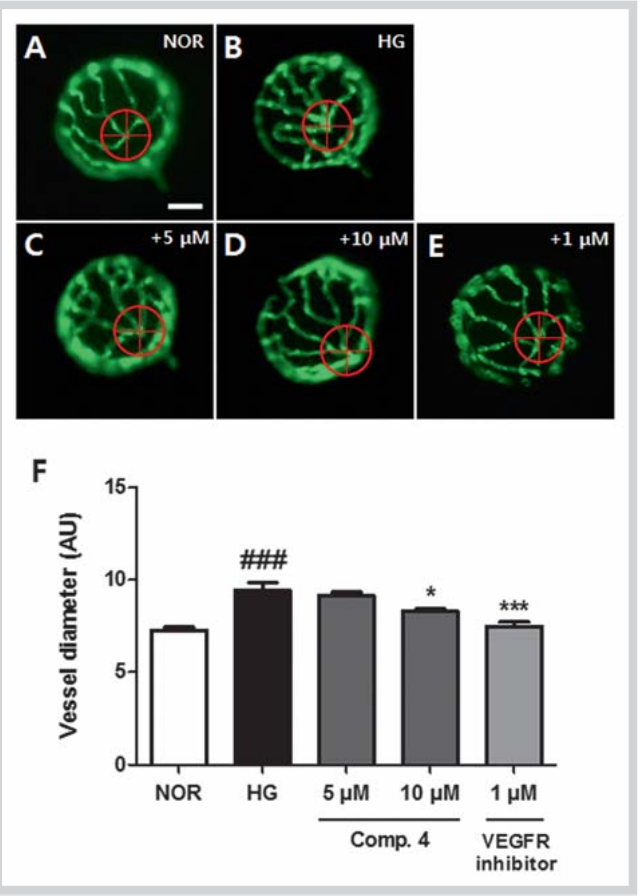

Fig. 4 Effect of compound **4** on dilation of hyaloid-retinal vessels from a high-glucose (HG)-induced diabetic retinopathy model. Hyaloid-retinal vessels of *flk*:EGFP transgenic zebrafish; **A** Untreated normal group (NOR). **B** HG-treated control group (HG). **C** 5 µM and **D** 10 µM compound **4** in the HG-treated group. **E** 1 µM VEGFR inhibitor in the HG-treated group. **F** Data are displayed as mean artificial units (AU) for vessel diameters. The diameters of hyaloid-retinal vessels were measured at locations proximal to the optic disc (red circle). Scale bar = 50 µm. The hyaloid vessel diameter of each lens was measured three times and the experiment was performed in triplicate. ###$P < 0.001$ vs. NOR, *$p < 0.05$ vs. HG, ***$p < 0.001$ vs. HG. (Color figure available online only.)

Fluorescence was visualized using the Olympus SZX16 stereomicroscope, and diameters were measured using ImageJ software. Experiments were performed in triplicate. VEGFR inhibitor (99.4 % purity; Calbiochem) was used as a positive control.

Statistical analysis

Statistical significance was assessed using one-way analysis of variance (ANOVA) and Dunnett's multiple comparison tests with the GraphPad 5.0 Prism software.

Acknowledgements

This research was supported by a grant (K15270 and K16270) from the Korea Institute of Oriental Medicine. The NMR experiment was performed by the Korea Basic Science Institute (KBSI).

Conflict of Interest

No conflict of interest exists.

References

1 *Wei M, Gaskill SP, Haffner SM, Stern MP.* Effect of diabetes and level of glycemia on all-cause and cardiovascular mortality: The San Antonio Heart Study. Diabetes Care 1998; 21: 1167–1172
2 *Laakso M.* Hyperglycemia and cardiovascular disease in type 2 diabetes. Diabetes 1999; 48: 937–942
3 *Brownlee M.* Biochemistry and molecular cell biology of diabetic complications. Nature 2001; 414: 813–820
4 *Takenaka K, Yamagishi S, Matsui T, Nakamura K, Imaizumi T.* Role of advanced glycation end products (AGEs) in thrombogenic abnormalities in diabetes. Curr Neurovasc Res 2006; 3: 73–77
5 *Kinoshita JH.* A thirty-year journey in the polyol pathway. Exp Eye Res 1990; 50: 567–573
6 *Morrison AD, Clements RS, Winegrad AI.* Effects of elevated glucose concentration on the metabolism of the aorta wall. J Clin Invest 1972; 51: 3114–3123
7 *Reddy VP, Beyaz A.* Inhibitors of the Maillard reaction and AGE breakers as therapeutics for multiple diseases. Drug Discov Today 2006; 11: 646–654
8 *Yabe-Nishimura C.* Aldose reductase in glucose toxicity: a potential target for the prevention of diabetic complications. Pharmacol Rev 1998; 50: 21–33
9 *Takeda K, Sakurawi K, Ishii H.* Components of the Lauraceae family – I. New lactonic compounds from *Litsea japonica*. Tetrahedron 1972; 28: 3757–3766
10 *Kozuka M.* On the alkaloid of *Litsea japonica* (Thumb.) Juss. I. Yakugaku Zasshi 1962; 82: 1567–1568
11 *Komae H, Hayashi N.* n-Paraffins from the leaves of three genera of Lauraceae. Phytochemistry 1971; 10: 3310
12 *Komae H, Hayashi N.* Terpenes from *Lindera erythrocarpa*. Phytochemistry 1972; 11: 853
13 *Miyamichi E, Nomura S.* Seed oil of Lauraceae I. Fatty acids from the seed oil of *Litsea japonica*. Yakugaku Zasshi 1953; 73: 169–170
14 *Ishikura N.* A survey of anthocyanins in fruits of some angiosperms, I. Bot Mag Tokyo 1975; 88: 41–45
15 *Kim E, Boo HJ, Hyun JH, Kim SC, Kang JI, Kim MK, Yoo ES, Kang HK.* The effect of *Litsea japonica* on the apoptosis induction of HL-60 leukemia cells. Yakhak Hoeji 2009; 53: 6–11
16 *Lee SY, Min BS, Kim JH, Lee J, Kim TJ, Kim CS, Kim YH, Lee HK.* Flavonoids from the leaves of *Litsea japonica* and their anti-complement activity. Phytother Res 2005; 19: 273–276
17 *Sohn E, Kim J, Kim CS, Lee YM, Jo K, Shin SD, Kim JH, Kim JS.* The extract of *Litsea japonica* reduced the development of diabetic nephropathy via the inhibition of advanced glycation end products accumulation in db/db mice. Evid Based Complement Alternat Med 2013; 2013: 769416
18 *Kim J, Kim CS, Sohn E, Lee YM, Jo K, Kim JS. Litsea japonica* extract inhibits aldose reductase activity and hyperglycemia-induced lenticular sorbitol accumulation in db/db mice. Evid Based Complement Alternat Med 2015; 2015: 747830
19 *Agrawal PK.* Carbone-13 NMR of Flavonoids. New York: Elsevier; 1989
20 *Kim YK, Kim YS, Choi SU, Ryu SY.* Isolation of flavonol rhamnosides from *Loranthus tanakae* and cytotoxic effect of them on human tumor cell lines. Arch Pharm Res 2004; 27: 44–47
21 *Lee SO, Choi SZ, Choi SU, Ryu SY, Lee KR.* Phytochemical constituents of the aerial parts from *Aster hispidus*. Nat Prod Sci 2004; 10: 335–340
22 *Piccinelli AL, Veneziano A, Passi S, De Simone F, Rastrelli L.* Flavonol glycosides from whole cottonseed by-product. Food Chem 2007; 100: 344–349
23 *Smite E, Pan H, Lundgren LN.* Lignan glycosides from inner bark of *Betula pendula*. Phytochemistry 1995; 40: 341–343
24 *Agrawal P, Rastogi R, Osterdahl B.* Carbon-13 NMR spectral analysis of dihydrobenzofuran lignans. Magn Reson Chem 1983; 21: 119–121
25 *Takeda Y, Mima C, Masuda T, Hirata E, Takuahi A, Otsuka H.* Glochidioboside, a glucoside of (7*S*,8*R*)-dihydrodehydrodiconiferyl alcohol from leaves of *Glochidion obovatum*. Phytochemistry 1998; 49: 2137–2139
26 *Miyase T, Ueno A, Takizawa N, Kobayashi H, Oguchi H.* Ionone and lignin glycosides from *Epimedium diphyllum*. Phytochemistry 1989; 28: 3483–3485
27 *Otsuka H, Hirata E, Shinzato T, Takeda Y.* Isolation of lignan glucosides and neolignan sulfate from the leaves of *Glochidion zeylanicum* (Gaertn) A. Juss. Chem Pharm Bull (Tokyo) 2000; 48: 1084–1086
28 *Nguyen DN, Ngo TT, Nguyen QL.* Highly sensitive fluorescence resonance energy transfer (FRET)-based nanosensor for rapid detection of clenbuterol. Adv Nat Sci Nanosci Nanotechnol 2012; 3: 035011
29 *Taguchi G, Shitchi Y, Shirasawa S, Yamamoto H, Hayashida N.* Molecular cloning, characterization, and downregulation of an acyltransferase that catalyzes the malonylation of flavonoid and naphthol glucosides in tobacco cells. Plant J 2005; 42: 481–491
30 *Lee IS, Kim IS, Lee YM, Lee Y, Kim JH, Kim JS.* 2″,4″-*O*-diacetylquercitrin, a novel advanced glycation end-product formation and aldose reductase inhibitor from *Melastoma sanguineum*. Chem Pharm Bull (Tokyo) 2013; 61: 662–665
31 *Brownlee M, Vlassara H, Kooney A, Ulrich P, Cerami A.* Aminoguanidine prevents diabetes-induced arterial wall protein cross-linking. Science 1986; 232: 1629–1632
32 *Jörgens K, Hillebrands JL, Hammes HP, Kroll J.* Zebrafish: a model for understanding diabetic complications. Exp Clin Endocrinol Diabetes 2012; 120: 186–187
33 *Tringali C.* Bioactive Compounds from natural Sources (Isolation, Characterization and biological Properties). London: Taylor & Francis Group; 2001
34 *Gao S, Hu M.* Bioavailability challenges associated with development of anticancer phenolics. Mini Rev Med Chem 2010; 10: 550–567